Ligand-based Computation of HIV-1 Integrase Inhibition Strength within a Series of β-ketoamide Derivatives

Frederik F. D. Daeyaert,* H. Maarten Vinkers, Marc R. de Jonge, Jan Heeres, Lucien M. H. Koymans, Paul J. Lewi, and Paul A. J. Janssen

Center for Molecular Design, Janssen Pharmaceutica N.V., Antwerpsesteenweg 37, B-2350 Vosselaar, Belgium

Internet Electronic Conference of Molecular Design **2003**, November 23 – December 6

Abstract

Motivation. A continuous demand exists for novel bioactive molecules. When a lead structure has been discovered and looks promising for further development, series of analogues will be made. Normally, the synthesis of many compounds is required to improve on the activity, or to keep good activity while optimising other properties of relevance. A computational model that accurately predicts the activity of derivatives before their synthesis is beneficial to the speed and cost of lead optimisation. It can be advantageous when such a model does not require geometrical information on the target protein structure.

Method. A conformational analysis was performed on 201 ketoamide ester derivatives that inhibit HIV integrase. The derivatives were aligned to the lowest energy conformer of the most potent inhibitor with the SEAL method. Five CoMSIA fields were computed for each compound taking into account steric, polarisability, charge, H-bond acceptor, and H-bond donor properties. A model for integrase-inhibitor interaction was derived by PLS regression. The predictivity of the model was tested by scrambling the data, leave-n-out experiments and applying the model to a ketoamide acid series of integrase inhibitors. In order to elucidate the binding mode of the inhibitors, the model was mapped on a crystal structure of the integrase enzyme.

Results. The CoMSIA model derived from the 201 ketoamide ester derivatives has an R^2 of 0.75. The resulting fields of the molecular properties required for strong inhibition can be qualitatively understood.

Scrambling the data prohibited the derivation of a predictive model. The models derived from 100 derivatives when applied to the remaining 101 compounds, resulted in a prediction with an absolute deviation of 0.28 $\log_{10}$ unit/compound. The accuracy of prediction when the model was applied to 74 ketoamide acids was 0.42 $\log_{10}$ unit/compound. Mapping the model onto the integrase enzyme did not lead to an obvious binding mode.

Conclusions. The predictivity of our model allows for guiding the synthesis of novel analogues. Our approach holds its predictive value when applied to a different series of inhibitors. The geometry of integrase-inhibitor binding is not very well understood at the present time, which emphasizes the advantages of an approach that does not require this knowledge for the design of novel active compounds.

Keywords. HIV; integrase; PLS; SEAL; CoMSIA; inhibition strength prediction; ligand-protein interaction.

Abbreviations and notations

AIDS, acquired immunodeficiency syndrome	MMFF, merck molecular force field
CoMSIA, comparative molecular similarity indices analysis	PDB, protein data bank
CPU, central processing unit	PLS, partial least squares
H-bond, hydrogen bond	QSAR, quantitative structure- activity relationships
HIV, human immunodeficiency virus	SEAL, steric and electrostatic alignment
IC_{50}, 50% inhibitory concentration	

* Correspondence author; phone: +32-14-442292; fax: +32-14-410503; E-mail: fdaeyaer@prdbe.jnj.com

1 INTRODUCTION

Integrase is an essential enzyme in the life cycle of HIV, the causative agent of AIDS. It is regarded as a promising target for anti-HIV compounds [1][2][3], but structure-based drug design efforts on HIV integrase have been hampered by lack of structural information on the exact binding mode of the available inhibitors. One structure of an inhibitor co-crystallised with the core domain of HIV integrase has been published [4]. We, and others [5][6], however, believe that the observed binding position of the inhibitor in this crystal structure is a result of crystal packing effects, and does not reflect the binding mode in an inhibited biological system. To enable reliable computation of inhibition strength anyhow, we have applied a QSAR approach that does not require structural information about the target enzyme: comparative molecular similarity indices analysis (CoMSIA) [7]. In this approach, similarity indices are calculated on a regular grid encompassing the space occupied by a set of aligned inhibitors. These similarity indices are the descriptors that are correlated to the observed activities. Due to the large number of similarity indices in comparison to the number of molecules, partial least squares regression is used to find the correlation between the similarity indices and the observed activities.

The first, and very critical, step in CoMSIA is the alignment of the molecules. We have used an approach based on the SEAL method, first described by Kearsley and Smith [8]. Aligning two molecules with the SEAL method is a computationally hard problem as it involves an optimisation in a high dimensional space formed by the torsional flexibility of the molecules plus the six rotation and translation degrees of freedom. We have alleviated this problem by predefining a pharmacophore model for HIV integrase inhibition from minimal knowledge about the enzyme, to constrain the search space. It has been demonstrated that the HIV integrase requires the presence of a divalent metal ion (Mg^{2+} or Mn^{2+}) to be functional [9]. Crystal structures of the core domain of HIV integrase with Mg^{2+} bound at the active site have been published [10][11]. Also, the activities of a number of classes of integrase inhibitors are dependent on the metal ion concentration. Therefore we hypothesize that the mechanism of action of these integrase inhibitors involves sequestration of the divalent ion. We started from this metal binding hypothesis to construct a simple alignment protocol, which consist of generating all possible bidentate metal complexes of an inhibitor, and then use the coordinates of the bound metal and the two coordinating inhibitor atoms to generate the alignments.

An important issue in deriving a QSAR using a large number of descriptors with respect to the number of activities is the risk of overfitting the data. We validate our model by 1- attempting to fit the scrambled data, 2- applying internal leave-one-out and leave-n-out cross validation, and 3- predicting the activities of an external data set.

Various other groups have reported QSAR studies on HIV integrase inhibitors, employing CoMSIA, CoMFA, and other approaches [12][13][14][15]. The picture that has emerged from these studies is that different classes of inhibitors have different mechanisms of action [16]. It is therefore difficult to compare these QSAR studies [15]. We have used the CoMSIA method on a series of β-ketoamide integrase inhibitors whose activities against recombinant HIV integrase have been experimentally determined. These data have recently been published by Katoh et al [17]. A ligand-based model that accurately predicts the activities within a series of inhibitors would be perfectly suited as input to a molecular design program [18] that accounts for the synthesizability of the generated compounds.

2 MATERIALS AND METHODS

The data set used to develop our model consists of 201 β-ketoamide ester derivatives with a pIC_{50} range between 5.05 and 8.39 (figure 1).

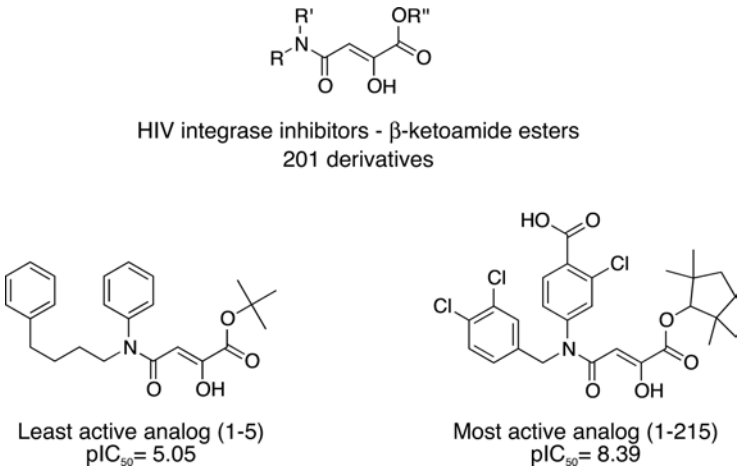

Figure 1. Structure of the β-ketoamide ester derivatives.

As a first step, the inhibitors are subjected to a conformational analysis using a genetic algorithm search strategy. The force field used is a modified version of the MMFF94 force field [19], extended with a directional hydrogen bond term and parameters for Mg. All conformers within 5 kcal/mole of the lowest energy conformer are retained. Next, for each conformer, all possible bidentate Mg^{2+} complexes are generated. This is accomplished by considering all combinations of possible coordinating atoms, and then rejecting the combinations that give rise to configurations where the distance between Mg and X -when Mg is placed at the center position between the coordinating atoms X- is too high or too low. Molecular mechanics energy minimization is applied to the remaining configurations and only the low energy configurations are retained.

As the basis for the alignment used in this study, the lowest energy conformation of the most potent compound was used. Note that this need not to be the biologically active conformation. The superposition of another molecule ('source') on the 'target' molecule is carried out by mapping the magnesium and two coordinating atoms of all conformers of the generated Mg complexes of the source onto the coordinates of the corresponding atoms of the target. Superposition without using the many other structural features that the derivatives in this study have in common, allows for application of the procedure to inhibitors of arbitrary structure, as long as they have a Mg^{2+} bidentate coordinating binding mode. The mapping is carried out by an implementation of Kabsch's algorithm for the superposition of two 3-dimensional vectors [20][21]. As the two coordinating atoms are equivalent, this superposition can be carried out in two ways for each Mg complex. For each superposition, the SEAL [8] similarity score S given in equation (1) with the target molecule is computed and the configuration with the highest score is retained.

$$S = \sum_{p=1}^{n_p} \sum_{i=1}^{n_s} \sum_{j=1}^{n_t} w^p f_i^p f_j^p e^{-\alpha r_{ij}^2} \tag{1}$$

In equation (1) n_p is the number of properties taken into consideration, n_s and n_t are the number of atoms in respectively the source and target molecule, f_i^p is the value of property p for atom i, w^p is a weight factor for property p, r_{ij} is the Euclidean distance between atom i and atom j, and α is an attenuation factor. We have used five properties for both the SEAL alignment and the CoMSIA analysis: the third power of the atomic radii as a steric property, the atomic polarizability used in the van der Waals term of the MMFF94 force field, the atomic partial charge derived from MMFF94, and the hydrogen bond acceptor and hydrogen bond donor strengths of the directional hydrogen bond term. The weights w^p are chosen such that the orders of magnitude of the maximal attainable values for the five properties are approximately equal (1, 5, 30, 5, and 5 respectively for the steric, polarizability, charge, hydrogen bond acceptor, and hydrogen bond donor properties). The attenuation factor was set to 0.3.

CoMSIA similarity fields were calculated on a three dimensional grid with a spacing of 1 Å encompassing the aligned molecules. On each grid point, five similarity indices S_g^p were calculated using equation (2).

$$S_g^p = \sum_{i=1}^{n_s} w^p f_i^p e^{-\alpha r_{ig}^2} \tag{2}$$

In equation (2), n_s is the number of atoms in the source molecule, f_i^p is the value of property p for atom i, w^p is the corresponding weight factor, r_{ig} is the Euclidean distance between atom i and grid point g, and α is an attenuation factor. The properties and their weight factors are identical to the one used for the SEAL alignment. The attenuation factor was set to 1.0, and only properties having a standard deviation over the 201 molecules on a grid point higher than a threshold value were retained.

The IC_{50} concentrations as reported [17] were converted to pIC_{50} values. To relate the activity of the molecules with the five property fields, partial least squares regression [22] was used. The predictivity of the derived model was assessed by leave-one-out and leave-n-out cross validation. For the different applications, both the explanatory R^2 and the correlation coefficient r^2 between observed and predicted activities are given. The explanatory R^2 is computed as

$$R^2 = 1 - \frac{\sum_{i=1}^{n}(y_i - \hat{y}_i)^2}{\sum_{i=1}^{n}(y_i - \bar{y})^2} \quad (3)$$

In equation (3) n is the number of datapoints, y_i is the observed value for datapoint i, $\hat{y}_i$ is the predicted value for datapoint i, and $\bar{y}$ denotes the mean of the observed values

To examine the model's behaviour on a different series of integrase inhibitors we used 74 β-ketoamide acid derivatives with a pIC_{50} range between 5.11 and 7.59 (figure 2).

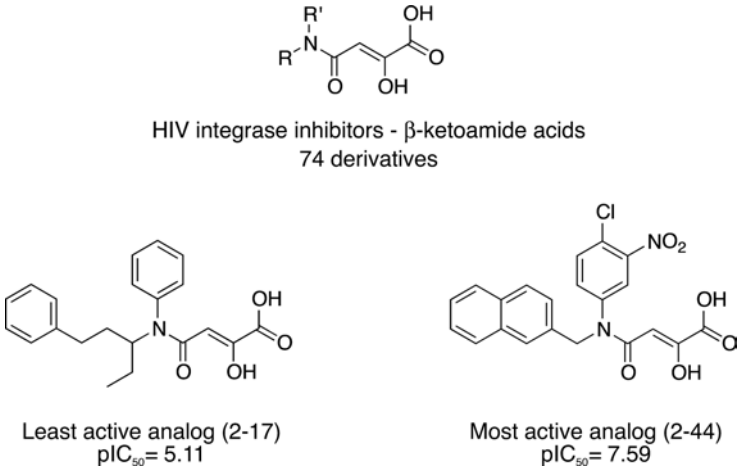

Figure 2. Structure of the β-ketoamide acid derivatives.

All calculations were carried out with in-house developed software using a Silicon Graphics R14000 CPU.

3 RESULTS AND DISCUSSION

3.1 CoMSIA model derived with PLS

A conformational search on the 201 β-ketoamide ester derivatives from the data set was carried out. The number of conformations generated varied from 16 to 366, with an average of 82 and a median of 70. The normalised SEAL scores of the alignment varied from 0.60 to 0.99, with an average and median of 0.81. The contributions of the five descriptors to the SEAL scores are listed

in table 1.

Property	Contribution
steric	0.656
polarisability	0.317
charge	0.010
H-bond acceptor	0.012
H-bond donor	0.005

Table 1. Normalised contributions of the five properties to the SEAL alignment.

As can be seen from table 1, the alignment is based almost exclusively on the steric and polarizability fields. This is attributable to the fact that the molecules considered are mostly apolar, with the exception of the metal chelating carbonyl groups.

Now that the molecules are aligned, a grid is defined encompassing the aligned set of molecules. This grid measures 31x27x25 Å, containing as many points. On each point the five properties are evaluated. The number of grid point/property combinations was reduced by applying a threshold onto the variance over the 201 inhibitors of each combination. In a series of test calculations, several values of this threshold (0.1, 0.01, and 0.001) were combined with several values of the attenuation factor α (0.1, 0.3, 1.0, and 2.0). Optimal values for fitted and predicted R^2 were obtained with a threshold value of 0.01 and an attenuation factor of 1.0. With this combination, 3968 grid point/property combinations were retained, which amounts to 3.8 % of the total (1188 steric, 1298 polarisability, 1113 charge, 220 hydrogen bond acceptor, and 149 hydrogen bond donor points). Lower values of the threshold did not deteriorate the results, but only led to an increase of data points. The predictivity of the PLS models derived was assessed using leave-one-out and leave-n-out cross validation. In the leave-n-out validation, half of the inhibitors was randomly selected as the training set. The other half of the inhibitors was then predicted with the model derived for this training set. The explanatory R^2 and predictive Q^2 values were calculated for one to five PLS components. This procedure was repeated 50 times and the explanatory R^2 and predictive Q^2 values were averaged. The results are summarized in table 2.

Components	R^2	Q^2 (loo)	R^2 (lno)*	Q^2 (lno)*
1	0.67	0.64	0.68	0.62
2	0.75	0.68	0.78	0.65
3	0.79	0.62	0.81	0.64
4	0.81	0.62	0.85	0.60
5	0.84	0.64	0.87	0.58

Table 2. Results of the internal validation of the CoMSIA/PLS models for the 201 β-ketoamide esters.

The best Q^2 was obtained with two PLS components. In figure 3 the observed pIC_{50} is plotted against the computed pIC_{50} for all 201 β-ketoamide esters. The R^2 for this fit is 0.75, the average absolute error is 0.27 log_{10} unit/compound and the error is less than one log_{10} unit for 98% of the inhibitors. When the activities of the 201 inhibitors are scrambled, the same analysis results in an average Q^2 of -0.04, indicating that the observed fits and predictions are not the result of chance correlations.

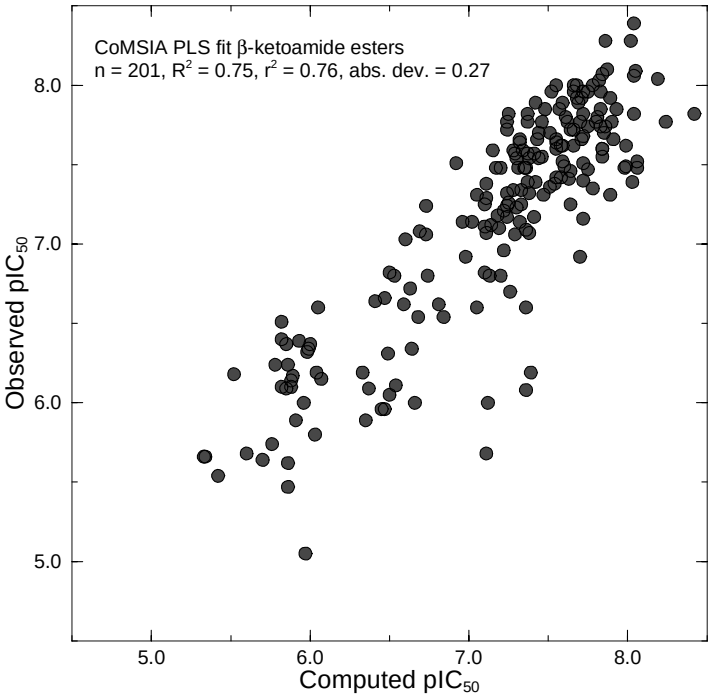

Figure 3. Observed against computed pIC_{50} for the 201 β-ketoamide esters.

* The figures for leave-n-out are averages over 50 trials.

Table 3 shows the normalized contribution of each of the five properties to the total predicted activities in this two component model. These contributions are calculated as sums over the 201 inhibitors and the five properties. On all gridpoints, the absolute value of the CoMSIA score for each property is multiplied with the corresponding PLS coefficient. Note that the contributions are different from the resulting ones in the alignment procedure.

Property	Contribution
steric	0.15
polarisability	0.36
charge	0.44
H-bond acceptor	0.03
H-bond donor	0.02

Table 3. Normalised contributions of the five properties to the activities of the 201 β-ketoamide esters.

Figures 4a and 4b on the following pages depict the magnitude of the PLS coefficients for the different properties. The steric and polarisability properties contribute to a high degree to the inhibition strength of a derivative. This can be seen from the number of contributions for these properties. The individual contributions of the charge are most pronounced. This implies that placement of a charged atom strongly influences the computed activity.

The orientation of the least active analog (figure 4b, compound 1-5) in the CoMSIA fields shows the absence of the right charge, acceptor, and donor properties, and shows the phenyl moiety of the phenylbutane substituent to be in the region of unfavourable steric and polarisability properties.

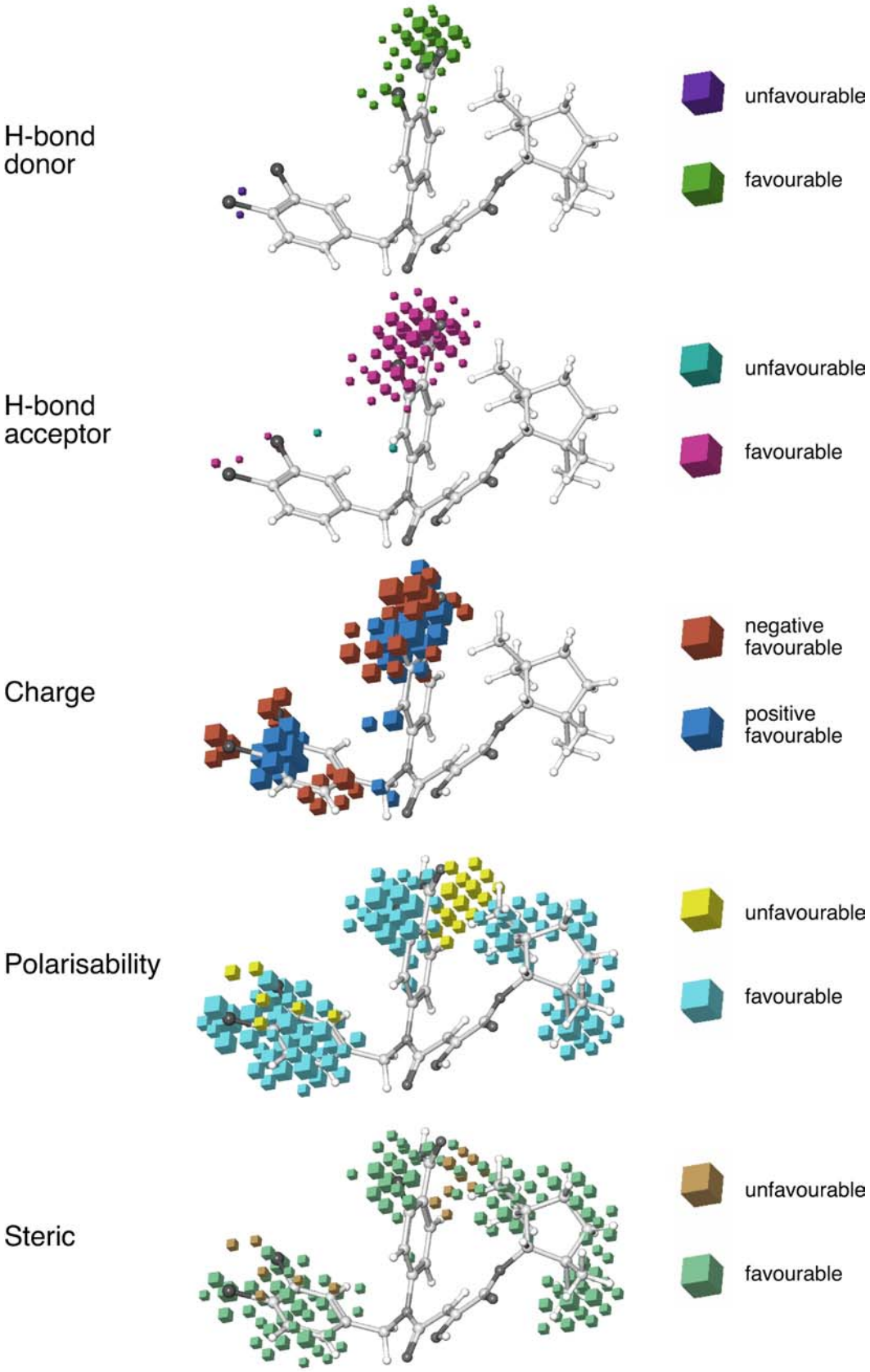

Figure 4a. CoMSIA fields around the most active analog. The size of the cubes for each property is proportional to the magnitude of the coefficient on the gridpoint in the model.

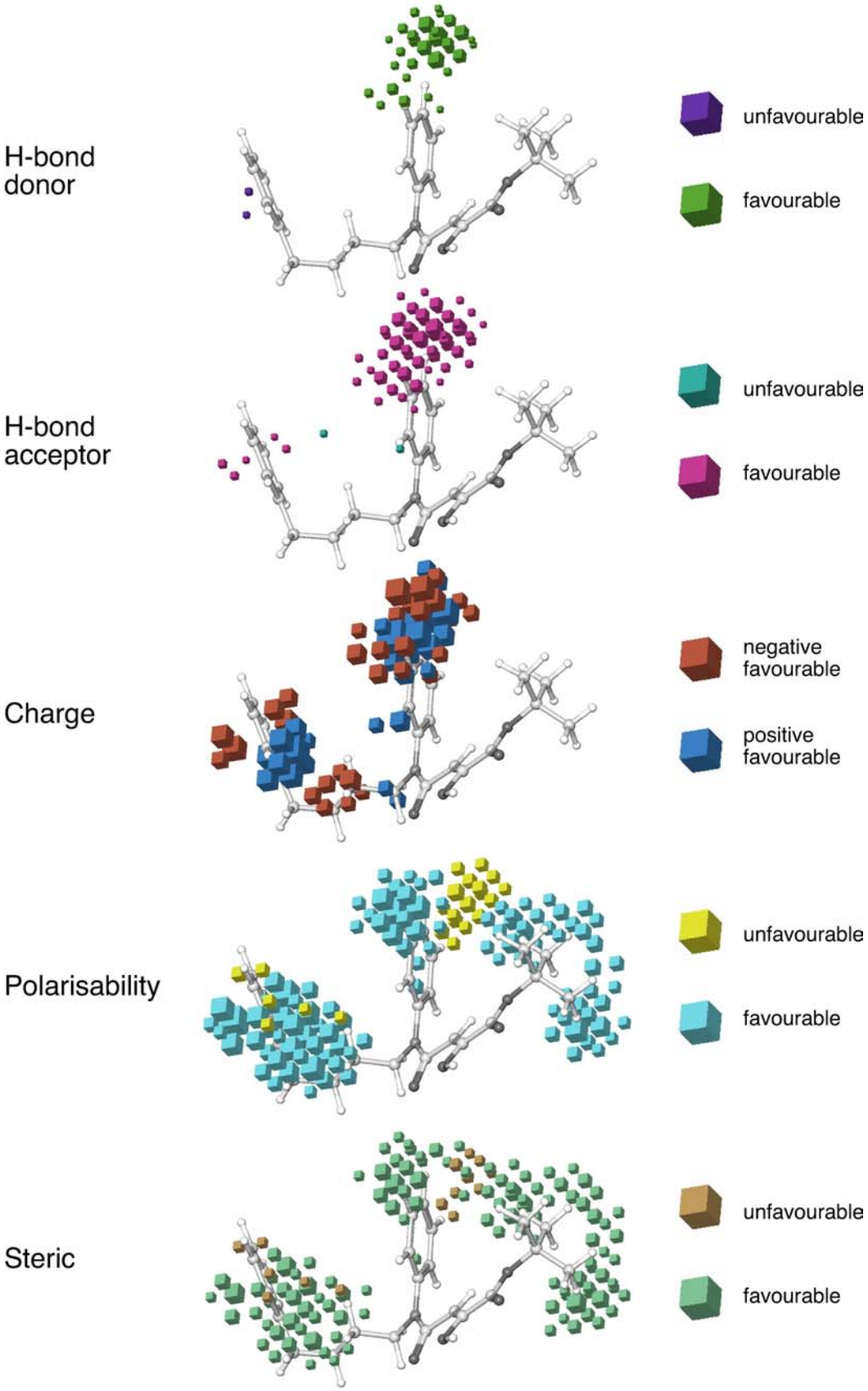

Figure 4b. CoMSIA fields around the least active analog. The size of the cubes for each property is proportional to the magnitude of the coefficient on the gridpoint in the model.

3.2 CoMSIA model predictions for β-ketoamide esters

Another way of illustrating the predictive power of the method is shown in figure 5, which gives predicted versus observed activities for 4 leave-n-out cross validation experiments. The prediction is remarkably robust for the choice of internal and external compounds. The high predictivity attained for the external sets demonstrates the merits of the CoMSIA model. We presume that the model benefits from the fact that all experimentally observed inhibition strengths are determined in one assay and are derived from an enzyme instead of a whole cell assay.

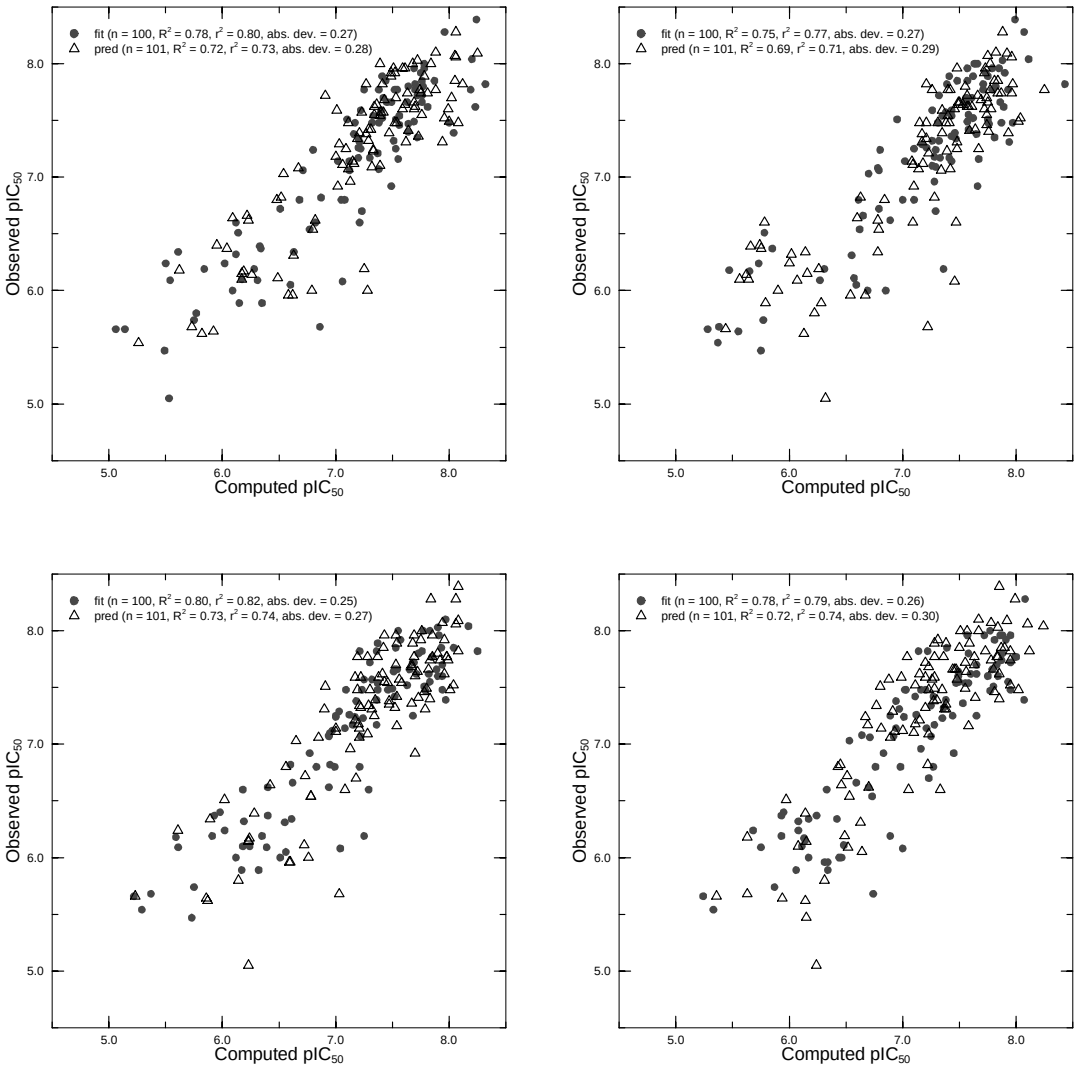

Figure 5. Observed against computed pIC_{50} for a fit of 100 β-ketoamide esters followed by prediction of the remaining 101 derivatives. The 101 analogs that are to be predicted were randomly chosen in a number of trials, the results of four different trials are depicted.

3.3 CoMSIA model predictions for β-ketoamide acids

We expect that the pharmacophore model we used for the alignment of the diketoamide inhibitors can be applied successfully to various classes of diketoaryl inhibitors, as they derive their inhibition from the same mechanism of action [23]. To test this hypothesis, we applied the ester-derived model to 74 acid analogues [17]. The results are shown in figure 6. An absolute deviation of 0.42 $\log_{10}$ unit/compound was obtained, which is a fair result. If only the ten highest predicted compounds were synthesized, the two most potent analogues would have been found. The difference between explanatory R^2 and squared correlation coefficient for the data reported in figure 6 is much higher than in figures 3 and 5. This suggests there may be a systematic difference between the two series which is not accounted for in the model. Other properties that do affect the potency of the compounds are not computed, but within one series these effects can be assumed as roughly being constant.

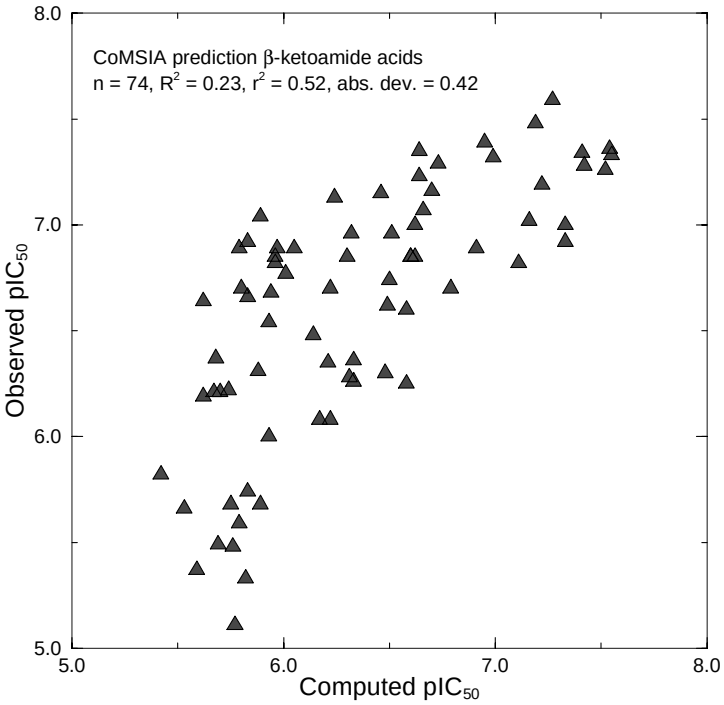

Figure 6. Observed against computed pIC_{50} for the prediction of the β-ketoamide acids.

3.4 CoMSIA model implications for integrase inhibitor binding

Given the two different binding hypotheses for integrase inhibitor binding, neither of which we used in the derivation of the CoMSIA model, it is interesting to see with which of these two our model matches best. To this end, we correlate the results of our model with the two different binding hypotheses. For the first binding mode, we construed a protein structure of the binding site complexed with Mg^{2+}. The structure was built from the 1BIS/1BIU/1BIZ [10] integrase crystal structures. The magnesium ion is coordinated by Asp 64 and Asp 116, and by two water molecules.

We have positioned the most active β-ketoamide ester (figure 1, compound 1-215) into the binding site of this structure to complete the octahedral coordination of the magnesium ion. First, we completed the octahedral coordination of the magnesium ion by adding two water molecules and carrying out a molecular mechanics minimization. Subsequently, we used the position of the two optimised water molecules and the magnesium ion to orient the ketoamide ester pharmacophore and thus to place the model. For the second binding mode, we used the crystal structure 1QS4 [4] – where an inhibitor is already bound– to place the model, by superimposing the hydroxypropenone moiety of the inhibitor on that of the crystal structure.

Figure 7 on the next page depicts the orientation of the CoMSIA fields with respect to the two systems. Neither the upper nor the lower complex looks completely plausible. In both systems, a number of favourable property points clash with sidechains of the protein. However, this could be caused by the way the model was placed in the binding site. A more rigorous approach to place the model would involve a docking of the inhibitor and possibly a minimisation step. In the upper structure, the favourable fields around the cyclopentane substituent make little interaction with the protein. Because the integrase crystal structure consists of the core only, protein atoms might be present here in the functional enzyme. Also, the inhibitor conformation used in this study may differ from the biologically active one. For instance, it might be a conformer that has its cyclopentane ring turned inwards. However, if the conformation used is attainable in all inhibitors, this will not affect the CoMSIA results. As an extreme example: should we have used the mirror image of the conformer, we would have arrived at exactly the same results. In the lower structure, the hydroxypropenone moiety of the inhibitor does not coordinate the magnesium ion, but it interacts with the Glu 152 and Lys 156 residues. The favourable H-bond donor and acceptor fields around the acid moiety of the benzoic acid substituent are in the same location as the magnesium ion, whereas the inhibitor in the original crystal structure fits without disturbing the ion. Summarizing, from our results it is difficult to decide which of the two binding hypotheses is more likely, or if any of the two is correct at all. It is remarkable that despite this uncertainty, the CoMSIA approach we have used is capable of accurately predicting the activity of the inhibitors.

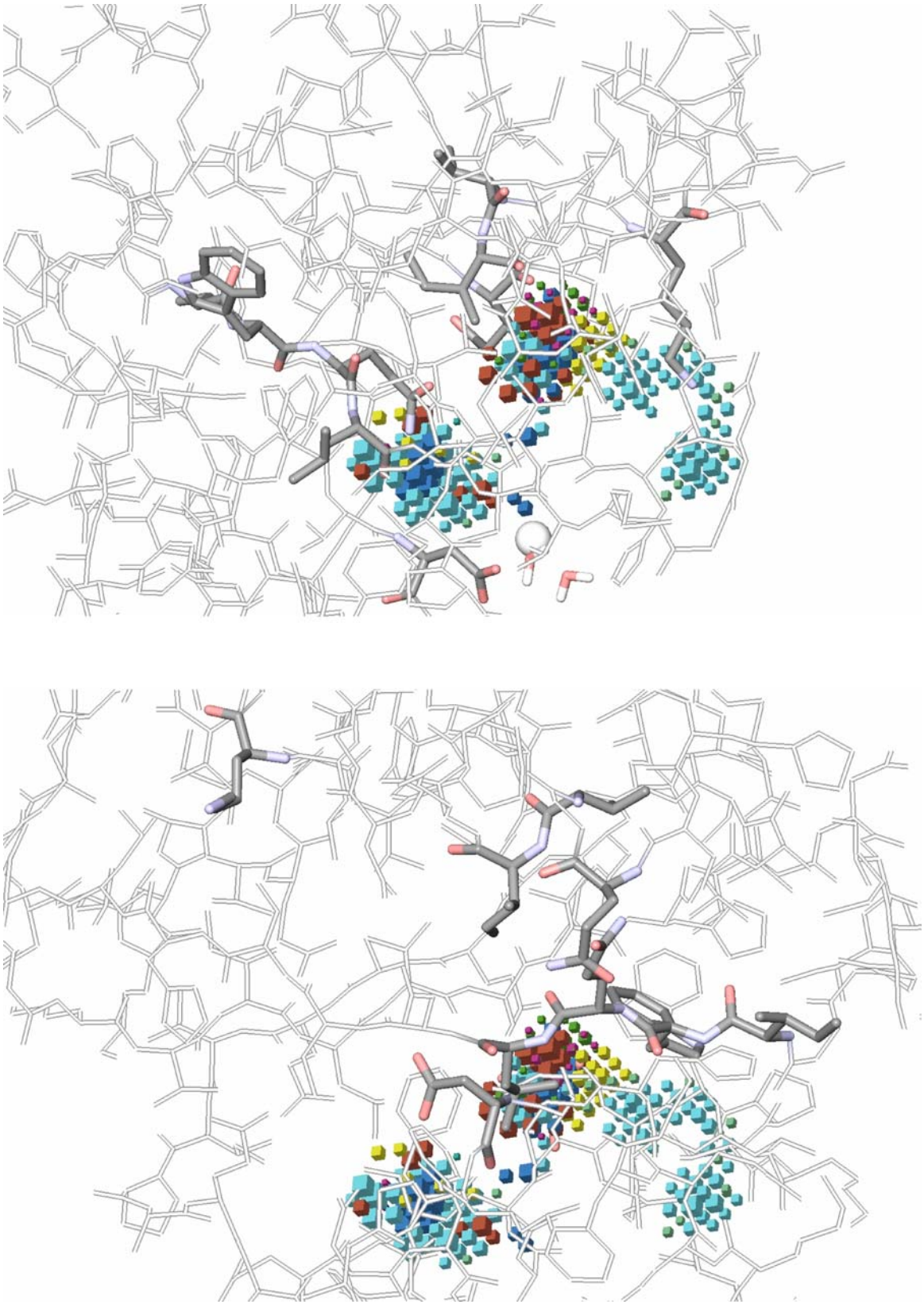

Figure 7. The position of the CoMSIA model with respect to the integrase enzyme in two binding mode hypotheses. The enzyme is shown as outline, with the sidechains of the binding site [6] in stick rendering. The template for the upper structure is 1BIS/1BIU/1BIZ [10], the template for the lower structure is 1QS4 [4].

4 CONCLUSIONS

The predictivity of our model allows for guiding the synthesis of novel analogues. Our approach holds its predictive value when applied to a different series. The geometry of integrase-inhibitor binding is not very well understood at the present time, which emphasizes the advantages of an approach that does not require this knowledge for the design of novel active compounds.

Acknowledgment

The authors gratefully acknowledge Joop H. van Lenthe for his review of the manuscript and Wim Abbeloos for building the molecules in the dataset.

Supplementary Material

An sdf-file containing the structures and activities of the 201 β-ketoamide ester derivatives and of the 74 β-ketoamide acid derivatives studied is available as supplementary material.

5 REFERENCES

[1] A. Pani, A.G. Loi, M. Mura, T. Marceddu, P. La Colla, and M.E. Marongiu, Targeting HIV: Old and New Players, *Curr. Drug Targets Infect. Disord.* **2002**, 2, 17-32.

[2] N. Neamati, Patented Small Molecule Inhibitors of HIV-1 Integrase: a 10-year Saga, *Expert Opin. Ther. Patents* **2002**, 12, 709-724.

[3] I..J. Chen, N. Neamati, and A.D. MacKerell Jr., Structure-Based Inhibitor Design Targeting HIV-1 Integrase, *Curr. Drug Targets Infect. Disord.* **2002**, 2, 217-234.

[4] Y. Goldgur, R. Craigie, G.H. Cohen, T. Fujiwara, T. Yoshinaga, T. Fujishita, H. Sugimoto, T. Endo, H. Murai, and D.R. Davies, Structure of the HIV-1 integrase catalytic domain complexed with an inhibitor: A platform for antiviral drug design, *Proc. Natl. Acad. Sci. U.S.A.* **1999**, 96, 13040-13043.

[5] C.A. Sotriffer, H. Ni, and J.A. McCammon, HIV-1 Integrase Inhibitor Interactions at the Active Site: Prediction of Binding Modes Unaffected by Crystal Packing, *J. Am. Chem. Soc.* **2000**, 122, 6136-6137.

[6] C.A. Sotriffer, H. Ni, and J.A. McCammon, Active Site Binding Modes of HIV-1 Integrase Inhibitors, *J. Med. Chem.* **2000**, 43, 4109-4117.

[7] G. Klebe, U. Abraham, and T. Mietzner, Molecular Similarity Indices in a Comparative Analysis (CoMSIA) of Drug Molecules to Correlate and Predict their Biological Activity, *J. Med. Chem.* **1994**, 37, 4130-4146.

[8] S.K. Kearsley and G.M. Smith, An Alternative Method for the Alignment of Molecular Structures: Maximizing Electrostatic and Steric Overlap, *Tetrahedron Computer Methodology* **1990**, 13, 615-633.

[9] J.A. Grobler, K. Stillmock, B. Hu, M. Witmer, P. Felock, A.S. Espeseth, A.Wolfe, M. Egbertson, M. Bourgeois, J. Melamed, J.S. Wai, S. Young, J. Vacca, and D.J. Hazuda, Diketo Acid Inhibitor Mechanism and HIV-1 Integrase: Implications for Metal Binding in the Active Site of Phosphotransferase Enzymes, *Proc. Natl. Acad. Sci. U.S.A.* **2002**, 99, 6661-6666.

[10] Y. Goldgur, F. Dyda, A.B. Hickman, T.M. Jenkins, R. Craigie, and D.R. Davies, Three New Structures of the Core Domain of HIV-1 Integrase: an Active Site that Binds Magnesium, *Proc. Natl. Acad. Sci. U.S.A.* **1998**, 95, 9150-9154.

[11] S. Maignan, J-P. Guilloteau, Q. Zhou-Liu, C. Clement-Mella, and V. Mikol, Crystal Structures of the Catalytic Domain of HIV-1 Integrase Free and Complexed with its Metal Cofactor: High Level of Similarity of the Active Site with Other Viral Integrases, *J. Mol. Biol.* **1998**, 282, 359-368.

[12] M.T. Makhija and V.M. Kulkarni, Eigen Value Analysis of HIV-1 Integrase Inhibitors, *J. Chem. Inf. Comput. Sci.* **2001**, 41, 1569-1577.

[13] M.T. Makhija and V.M. Kulkarni, Molecular Electrostatic Potentials as Input for the Alignment of HIV-1 Integrase Inhibitors in 3D QSAR, *J. Comput. Aided Mol. Des.* **2001**, 15, 961-978.

[14] J.K. Buolamwini and H. Assefa, CoMFA and CoMSIA 3D QSAR and Docking Studies on Conformationally-Restrained Cinnamoyl HIV-1 Integrase Inhibitors: Exploration of a Binding Mode at the Active Site, *J. Med. Chem.* **2002**, 45, 841-852.

[15] H. Yuan and A.L. Parrill, QSAR Studies of HIV-1 Integrase Inhibition, *Bioorg. Med. Chem.* **2002**, 10, 4169-4183.

[16] A.L. Parrill, HIV-1 Integrase Inhibition: Binding Sites, Structure Activity Relationships and Future Perspectives, *Curr. Med. Chem.* **2003**, 10, 1811-1824.
[17] S. Katoh, S. Miyazaki, and N. Habuka, Preparation of β-Ketoamide Compounds as HIV Integrase Inhibitors, 2003, WO 2003016266.
[18] H.M. Vinkers, M.R. de Jonge, F.F.D. Daeyaert, J. Heeres, L.M.H. Koymans, J.H. van Lenthe, P.J. Lewi, H. Timmerman, K. Van Aken, and P.A.J. Janssen, SYNOPSIS: SYNthesize and OPtimize System in Silico, *J. Med. Chem.* **2003**, 46, 2765-2773.
[19] T.A. Halgren, Merck Molecular Force Field. I. Basis, Form, Scope, Parametrization and Performance of MMFF94, *J. Comput. Chem* **1996**, 17, 490-519.
[20] W. Kabsch, A Discussion of the Solution for the Best Rotation to Relate Two Sets of Vectors, *Acta Cryst.* **1978**, A34, 827-828.
[21] D.J. Heisterberg, Unpublished results.
[22] B.G.M Vandeginste, D.L. Massart, L.C.M. Buydens, S. De Jong, P.J. Lewi, and J. Smeyers-Verbeke, Handbook of Chemometrics and Qualimetrics: Part B, Elsevier, Amsterdam, 1998, pp. 331-342.
[23] G.C.G. Pais and T.R. Burke Jr., Novel Aryl Diketo-containing Inhibitors of HIV-1 Integrase, *Drugs of the Future* **2002**, 27, 1101-1111.